Eur. Phys. J. B **6**, 257–271 (1998)

THE EUROPEAN PHYSICAL JOURNAL B

Envelope solitary waves on two-dimensional lattices with in-plane displacements

Y. Gaididei[1], R. Huß[2], and F.G. Mertens[2,a]

[1] Institute for Theoretical Physics, 252143 Kiev, Ukraine
[2] Physikalisches Institut, Universität Bayreuth, 95440 Bayreuth, Germany

Received: 4 December 1997 / Revised: 6 June 1998 / Accepted: 7 July 1998

Abstract. We investigate envelope solitary waves on square lattices with two degrees of freedom and nonlinear nearest and next-nearest neighbor interactions. We consider solitary waves which are localized in the direction of their motion and periodically modulated along the perpendicular direction. In the quasi-monochromatic approximation and low-amplitude limit a system of two coupled nonlinear Schrödinger equations (CNLS) is obtained for the envelopes of the longitudinal and transversal displacements. For the case of bright envelope solitary waves the solvability condition is discussed, also with respect to the modulation. The stability of two special solution classes (type-I and type-II) of the CNLS equations is tested by molecular dynamics simulations. The shape of type-I solitary waves does not change during propagation, whereas the width of type-II excitations oscillates in time.

PACS. 03.40.Kf Waves and wave propagation: general mathematical aspects – 63.20.Ry Anharmonic lattice modes – 62.20.Pw Mechanical properties of solids

1 Introduction

The dynamical and thermodynamical properties of anharmonic chains have been studied both analytically and numerically by many authors over the last three decades (for reviews, see *e.g.* [1–6]). It was shown that these anharmonic chains can bear both kink-like excitations which in the long-wave approximation are solutions of a Boussinesq type of equation and envelope solitary waves which are described by a nonlinear Schrödinger (NLS) type of equation. They are very robust and propagate without energy loss, and their collisions are almost elastic even beyond the range of the continuum approximation.

However, the studies of nonlinear excitations in two-dimensional anharmonic lattices are much less developed. The main attention has been paid to the investigation of nonlinear excitations in models of two-dimensional lattices with only one scalar degree of freedom per lattice site. Eilbeck [7] and Duncan *et al.* [8] studied a strongly anisotropic two-dimensional lattice which is described by the Kadomtsev-Petviashvili equation in the continuum limit. Druzhinin and Ostrovskii [9] considered nonlinear excitations in quadratic and hexagonal lattices with a cubic anharmonicity and showed the existence of cylindrical solitary wave fronts. Kivshar [10] investigated the influence of nonlinearity on shear horizontal elastic waves and showed the possibility to observe bright and dark envelope solitary waves. Pouget *et al.* [11] studied nonlinear properties of two-dimensional anharmonic lattices on periodical substrates and investigated energy localization and gap local pulses. Bonart and coauthors [12] studied anharmonic excitations which are localized at the surface of two- and three-dimensional lattices.

Until recently there have been only a few analytical and numerical studies of two-dimensional lattice-dynamical models with two-component displacement vectors. Gaididei *et al.* [13] showed that the propagation of axi-symmetric nonlinear acoustic pulses is governed by a radial Boussinesq equation which is a cylindrical analogue of the one-dimensional Boussinesq equation. Bonart *et al.* [12] considered intrinsic localized anharmonic modes at an edge of a 3-dimensional crystal taking into account realistic interatomic interaction potentials and proved their stability over times much longer the vibrational period. Eilbeck [14] found in a two-dimensional hexagonal lattice model localized propagating breathers. Quite recently we presented the results of investigations of solitary excitations on square lattices with nonlinear interactions between nearest and next-nearest neighbours taking into account anharmonic interactions of third and fourth order [15]. We searched for solitary waves depending only on one space variable and in the continuum limit we obtained a Zakharov-like set of two coupled nonlinear partial differential equations for the longitudinal and transversal displacements. We got localized solutions which were used as initial conditions for computer simulations. For the case of Morse interatomic potentials we found solitary waves

[a] e-mail: franz.mertens@theo.phy.uni-bayreuth.de

which are a combination of a kink and an envelope solitary wave for the longitudinal and transversal displacements, respectively. The goal of this paper is to expand on the results of [15], taking into account the dependence of atomic displacements on *two* spatial variables. The approach of the present work is to obtain analytical expressions for solitonic excitations in square lattices with in-plane displacements using the quasicontinuum approximation and compare these expressions with the results of numerical simulations.

The remainder of this paper is outlined as follows. In Section 2 we introduce our model which is a two-dimensional quadratic lattice model with anharmonic interactions of third and fourth order. We consider the effect of nonlinearity on the propagation of two-dimensional elastic waves. In the quasi-monochromatic approximation and for low-amplitude modulation we show that the basic equations governing the lattice dynamics are reduced to a system of coupled nonlinear Schrödinger equations in the slow variables. In Section 3 we deal with numerical simulations using as initial conditions analytical solutions obtained from the system of nonlinear Schrödinger equations. Section 4 is devoted to a summary and concluding remarks. In the Appendix we present an alternative derivation of the governing equations based on the multiple-scale perturbation method.

2 System and equations of motion

We consider a quadratic two-dimensional lattice of particles of mass m ($m = 1$) with lattice spacing a ($a = 1$). The displacement of the nth particle from equilibrium is $\mathbf{u}(\mathbf{n}, t)$ where $\mathbf{u} = (u_x, u_y)$ as well as $\mathbf{n} = (n_x, n_y)$ are two-dimensional vectors. In the following, to simplify some formulas we will denote u_x also as u_1, u_y as u_2, *etc.* The Lagrangian of our system is given by

$$\mathcal{L} = T - U\,. \tag{1}$$

Here

$$T = \frac{1}{2}\sum_{\mathbf{n}}\sum_{\alpha}\dot{u}_\alpha(n)\dot{u}_\alpha(n) \tag{2}$$

is the kinetic energy,

$$U = \frac{1}{2}\sum_{\mathbf{n}}\sum_{\boldsymbol{\Delta}} V_\Delta(|\boldsymbol{\Delta} + \mathbf{u}(\mathbf{n}) - \mathbf{u}(\mathbf{n}-\boldsymbol{\Delta})|) - V_\Delta(|\boldsymbol{\Delta}|) \tag{3}$$

is the the potential energy of the system.

$V_\Delta(|\mathbf{r}|)$ is the interaction potential of two atoms and is a function of their separation $|\mathbf{r}|$ only, $\boldsymbol{\Delta} = (\Delta_x, \Delta_y)$ being the vector which connects an atom with its nearest ($\boldsymbol{\Delta} = (\pm 1, 0), (0, \pm 1), \Delta = 1$) and next-nearest neighbors ($\boldsymbol{\Delta} = (1,1), (1,-1), (-1,1), (-1,-1)$, $\Delta = \sqrt{2}$). For stability reasons we include next nearest neighbor interactions from the very beginning in the interatomic potentials[1].

Expanding the potential function:

$$V_\Delta\left(|\boldsymbol{\Delta} + \mathbf{u}(\mathbf{n}) - \mathbf{u}(\mathbf{n}-\boldsymbol{\Delta})|\right)$$

into a Taylor series up to fourth order of $\mathbf{u}(\mathbf{n})$ we get

$$U = U_2 + U_3 + U_4. \tag{4}$$

Here

$$U_2 = \frac{1}{4}\sum_{\mathbf{n}}\sum_{\boldsymbol{\Delta}}\sum_{\alpha,\beta} V_{\alpha\beta}(\boldsymbol{\Delta}) w_\alpha(\mathbf{n}, \boldsymbol{\Delta}) w_\beta(\mathbf{n}, \boldsymbol{\Delta}) \tag{5}$$

with

$$V_{\alpha\beta}(\boldsymbol{\Delta}) = K_\Delta \frac{\Delta_\alpha \Delta_\beta}{\Delta^2} \tag{6}$$

is the harmonic part of the potential energy,

$$U_3 = \frac{1}{6}\sum_{\mathbf{n}}\sum_{\boldsymbol{\Delta}}\sum_{\alpha,\beta,\gamma} V_{\alpha\beta\gamma}(\boldsymbol{\Delta}) w_\alpha(\mathbf{n}, \boldsymbol{\Delta}) w_\beta(\mathbf{n}, \boldsymbol{\Delta}) w_\gamma(\mathbf{n}, \boldsymbol{\Delta}) \tag{7}$$

with

$$V_{\alpha\beta\gamma}(\boldsymbol{\Delta}) = \frac{1}{2}\left(\frac{3K_\Delta}{\Delta} - L_\Delta\right)\frac{\Delta_\alpha\Delta_\beta\Delta_\gamma}{\Delta^3} - \frac{1}{2}\frac{K_\Delta}{\Delta}\left(\delta_{\alpha\beta}\frac{\Delta_\gamma}{\Delta} + \delta_{\alpha\gamma}\frac{\Delta_\beta}{\Delta} + \delta_{\gamma\beta}\frac{\Delta_\alpha}{\Delta}\right) \tag{8}$$

is the third-order anharmonicity term, and

$$U_4 = \frac{1}{8}\sum_{\mathbf{n}}\sum_{\boldsymbol{\Delta}}\sum_{\alpha,\beta,\gamma,\delta} V_{\alpha\beta\gamma\delta}(\boldsymbol{\Delta}) w_\alpha(\mathbf{n}, \boldsymbol{\Delta}) \times w_\beta(\mathbf{n}, \boldsymbol{\Delta}) w_\gamma(\mathbf{n}, \boldsymbol{\Delta}) w_\delta(\mathbf{n}, \boldsymbol{\Delta}) \tag{9}$$

with

$$\begin{aligned} V_{\alpha\beta\gamma\delta}(\boldsymbol{\Delta}) = {} & \left(\frac{5}{2}\frac{K_\Delta}{\Delta^2} - \frac{L_\Delta}{\Delta} + \frac{1}{6}M_\Delta\right)\frac{\Delta_\alpha\Delta_\beta\Delta_\gamma\Delta_\delta}{\Delta^4} \\ & + \frac{1}{6}\left(\frac{L_\Delta}{\Delta} - 3\frac{K_\Delta}{\Delta^2}\right)\left(\frac{\Delta_\alpha\Delta_\beta}{\Delta^2}\delta_{\gamma\delta} + \frac{\Delta_\delta\Delta_\beta}{\Delta^2}\delta_{\gamma\alpha} + \frac{\Delta_\gamma\Delta_\delta}{\Delta^2}\delta_{\alpha\beta} \right. \\ & \left. + \frac{\Delta_\gamma\Delta_\beta}{\Delta^2}\delta_{\alpha\delta} + \frac{\Delta_\alpha\Delta_\delta}{\Delta^2}\delta_{\gamma\beta} + \frac{\Delta_\alpha\Delta_\gamma}{\Delta^2}\delta_{\delta\beta}\right) \\ & + \frac{1}{6}\frac{K_\Delta}{\Delta^2}\left(\delta_{\alpha\beta}\delta_{\gamma\delta} + \delta_{\alpha\gamma}\delta_{\beta\delta} + \delta_{\alpha\delta}\delta_{\gamma\beta}\right) \end{aligned} \tag{10}$$

is the fourth-order anharmonicity term. In equations (4–10) the notations

[1] A quadratic lattice with pure nearest neighbor interactions is instable, *i.e.* the lattice can be distorted to a one dimensional chain without applying any force.

$$\frac{1}{2}\,\omega_\mu^2(\mathbf{k}) = K_1\left(\sin^2(\tfrac{k_x}{2})+\sin^2(\tfrac{k_y}{2})\right) + K_{\sqrt{2}}\left(\sin^2(\tfrac{k_x+k_y}{2})+\sin^2(\tfrac{k_x-k_y}{2})\right) \tag{17}$$
$$-(-1)^\mu\sqrt{K_1^2\left(\sin^2(\tfrac{k_x}{2})-\sin^2(\tfrac{k_y}{2})\right)^2 + K_{\sqrt{2}}^2\left(\sin^2(\tfrac{k_x+k_y}{2})-\sin^2(\tfrac{k_x-k_y}{2})\right)^2}$$

$$\begin{aligned} w_\alpha(\mathbf{n},\boldsymbol{\Delta}) &= u_\alpha(\mathbf{n}-\boldsymbol{\Delta}) - u_\alpha(\mathbf{n}),\\ K_\Delta &= \frac{\mathrm{d}^2}{\mathrm{d}x^2}V_\Delta(x)\Big|_{x=\Delta}\\ L_\Delta &= \frac{\mathrm{d}^3}{\mathrm{d}x^3}V_\Delta(x)\Big|_{x=\Delta}\\ M_\Delta &= \frac{\mathrm{d}^4}{\mathrm{d}x^4}V_\Delta(x)\Big|_{x=\Delta} \end{aligned} \tag{11}$$

were used.

From the Lagrangian (1) we obtain the equations of motion

$$\begin{aligned} \ddot{u}_\alpha(\mathbf{n}) = &\sum_{\boldsymbol{\Delta},\beta} V_{\alpha\beta}(\boldsymbol{\Delta})w_\beta(\mathbf{n},\boldsymbol{\Delta}) \\ &+ \sum_{\boldsymbol{\Delta},\beta,\gamma} V_{\alpha\beta\gamma}(\boldsymbol{\Delta})w_\beta(\mathbf{n},\boldsymbol{\Delta})w_\gamma(\mathbf{n},\boldsymbol{\Delta}) \\ &+ \sum_{\boldsymbol{\Delta},\beta,\gamma,\delta} V_{\alpha\beta\gamma\delta}(\boldsymbol{\Delta})w_\beta(\mathbf{n},\boldsymbol{\Delta})w_\gamma(\mathbf{n},\boldsymbol{\Delta})w_\delta(\mathbf{n},\boldsymbol{\Delta}). \end{aligned} \tag{12}$$

The transformation

$$u_\alpha(\mathbf{n}) = \frac{1}{\sqrt{N}}\sum_{\mathbf{k}}\sum_{\nu} e^{i\mathbf{kn}}T_{\alpha\nu}(\mathbf{k})\zeta_\nu(\mathbf{k}) \tag{13}$$

with $\mathbf{k}=(k_x,k_y)$ being a two-dimensional wave vector,

$$\begin{aligned} T_{11}(\mathbf{k}) &= \;\; T_{22}(\mathbf{k}) = \cos(\eta(\mathbf{k}))\\ T_{21}(\mathbf{k}) &= -T_{12}(\mathbf{k}) = \sin(\eta(\mathbf{k})) \end{aligned} \tag{14}$$

where $N=N_1N_2$ is the number of particles in the lattice,

$$\tan(\eta(\mathbf{k})) = \frac{A_d(\mathbf{k})}{A_p(\mathbf{k})+\sqrt{A_p^2(\mathbf{k})+A_d^2(\mathbf{k})}} \tag{15}$$

and

$$\begin{aligned} A_p(\mathbf{k}) &= K_1\left(\sin^2(\tfrac{k_x}{2})-\sin^2(\tfrac{k_y}{2})\right)\\ A_d(\mathbf{k}) &= K_{\sqrt{2}}\left(\sin^2(\tfrac{k_x+k_y}{2})-\sin^2(\tfrac{k_x-k_y}{2})\right) \end{aligned} \tag{16}$$

diagonalizes the harmonic part of the Lagrangian $\mathcal{L}_0 = T-U_2$. The eigenfrequencies are defined by the expressions

See equation (17) above.

In the small-$|\mathbf{k}|$ limit the frequency $\omega_1(\mathbf{k})$ belongs to a longitudinal acoustic wave while $\omega_2(\mathbf{k})$ belongs to a transversal one.

We will consider nonlinear excitations with frequencies in a small interval around one of the harmonic frequencies of the system, say

$$\omega = \omega_\mu(\mathbf{q}) \tag{18}$$

where $\mu=1,2$ is a fixed index and $\mathbf{q}$ is an arbitrary wave vector in the first Brillouin zone. To put it in another way, we will consider envelope solitary waves with carrier frequency (18) and carrier wave vector $\mathbf{q}$.

To obtain effective equations which describe spatial and temporal variations of nonlinear excitations in the chosen frequency interval we used two approaches. The first one is similar to the method used in [12]. It is rather heuristic but faster than the second approach which is based on the multiple-scale analysis (see Appendix).

Let us expand the displacement $u_\alpha(\mathbf{n},t)$ into a series where we separate the fast and slow time dependencies

$$u_\alpha(\mathbf{n},t) = \sum_{l=-\infty}^{\infty} e^{-il\omega t}u_\alpha^{(l)}(\mathbf{n},t) \tag{19}$$

where $u_\alpha^{(l)}(\mathbf{n},t) = \left(u_\alpha^{(-l)}(\mathbf{n},t)\right)^*$. The first harmonics $u_\alpha^{(\pm1)}(\mathbf{n},t)$ are responsible for the nonlinear properties of the system in the frequency interval around (18). Taking into account that the star of the vector $\mathbf{q}$ (see *e.g.* [16]) consists of the following four vectors

$$\begin{aligned} \mathbf{q} &\equiv (q_x,q_y) & \mathbf{q}' &\equiv (q_x,-q_y)\\ -\mathbf{q} & & -\mathbf{q}' & \end{aligned} \tag{20}$$

we can write the expression for $u_\alpha^{(1)}(\mathbf{n},t)$ in the form

$$\begin{aligned} u_\alpha^{(1)}(\mathbf{n},t) = &\, e^{i\mathbf{qn}}\frac{1}{\sqrt{N}}\sum_{\mathbf{k}} e^{i\mathbf{kn}}T_{\alpha\mu}(\mathbf{k}+\mathbf{q})\phi_\mu(\mathbf{k},t) \\ &+ e^{i\mathbf{q}'\mathbf{n}}\frac{1}{\sqrt{N}}\sum_{\mathbf{k}} e^{i\mathbf{kn}}T_{\alpha\mu}(\mathbf{k}+\mathbf{q}')\psi_\mu(\mathbf{k},t) \end{aligned} \tag{21}$$

where the amplitudes $\psi_\mu(\mathbf{k},t)$ and $\phi_\mu(\mathbf{k},t)$ are the Fourier components of the envelope functions

$$\begin{aligned} \Phi_\mu(\mathbf{n},t) &= \frac{1}{\sqrt{N}}\sum_{\mathbf{k}} e^{i\mathbf{kn}}\phi_\mu(\mathbf{k},t),\\ \Psi_\mu(\mathbf{n},t) &= \frac{1}{\sqrt{N}}\sum_{\mathbf{k}} e^{i\mathbf{kn}}\psi_\mu(\mathbf{k},t). \end{aligned} \tag{22}$$

They are defined only for small $|\mathbf{k}|$ and therefore the envelope functions $\Phi(\mathbf{n},t)$ and $\Psi(\mathbf{n},t)$ are slowly varying functions of $\mathbf{n}$. Using equation (22) one can approximately

write instead of equation (21)

$$u_\alpha^{(1)}(\mathbf{n},t) = e^{i\mathbf{qn}}\left(T_{\alpha\mu}(\mathbf{q}) - i\frac{\partial T_{\alpha\mu}(\mathbf{q})}{\partial \mathbf{q}}\frac{\partial}{\partial \mathbf{n}}\right)\Phi_\mu(\mathbf{n},t) \quad (23)$$
$$+e^{i\mathbf{q'n}}\left(T_{\alpha\mu}(\mathbf{q'}) - i\frac{\partial T_{\alpha\mu}(\mathbf{q'})}{\partial \boldsymbol{q'}}\frac{\partial}{\partial \mathbf{n}}\right)\Psi_\mu(\mathbf{n},t).$$

Inserting equation (19) into the equations of motion and keeping terms (12) up to the second order of $u^{(1)}(\mathbf{n},t)$ we obtain the following set of coupled equations

$$\partial_t^2 u_\alpha^{(0)}(\mathbf{n},t) = \sum_{\boldsymbol{\Delta},\beta} V_{\alpha\beta}(\boldsymbol{\Delta}) w_\beta^{(0)}(\mathbf{n},t) + 2\sum_{\boldsymbol{\Delta},\beta,\gamma} V_{\alpha\beta\gamma}(\boldsymbol{\Delta}) w_\beta^{(-1)}(\mathbf{n},t) w_\gamma^{(1)}(\mathbf{n},t) \quad (24)$$

$$(\partial_t^2 - \omega^2 - 2i\omega\partial_t)u^{(1)}(\mathbf{n},t) = \sum_{\boldsymbol{\Delta},\beta} V_{\alpha\beta}(\boldsymbol{\Delta}) w_\beta^{(1)}(\mathbf{n},t) \quad (25)$$
$$+2\sum_{\boldsymbol{\Delta},\beta,\gamma} V_{\alpha\beta\gamma}(\boldsymbol{\Delta})\left(w_\beta^{(0)}(\mathbf{n},t) w_\gamma^{(1)}(\mathbf{n},t) + w_\beta^{(-1)}(\mathbf{n},t) w_\gamma^{(2)}(\mathbf{n},t)\right)$$
$$+3\sum_{\boldsymbol{\Delta},\beta,\gamma,\delta} V_{\alpha\beta\gamma\delta}(\boldsymbol{\Delta}) w_\beta^{(1)}(\mathbf{n},t) w_\gamma^{(1)}(\mathbf{n},t) w_\delta^{(-1)}(\mathbf{n},t);$$

$$-4\omega^2 u_\alpha^{(2)}(\mathbf{n},t) = \sum_{\boldsymbol{\Delta},\beta} V_{\alpha\beta}(\boldsymbol{\Delta}) w_\beta^{(2)}(\mathbf{n},t) + \sum_{\boldsymbol{\Delta},\beta,\gamma} V_{\alpha\beta\gamma}(\boldsymbol{\Delta}) w_\beta^{(1)}(\mathbf{n},t) w_\gamma^{(1)}(\mathbf{n},t). \quad (26)$$

Equations (24–26) were obtained using the following approximations;

i) The harmonics $u^{(l)}(\mathbf{n},t)$ with $|l| \geq 3$ were neglected because of their smallness (our numerical simulations show that the third harmonic is 10 times smaller than the second one).
ii) Both time derivatives on the right-hand-side of equation (26) were neglected because we will consider only excitations for which $2\omega_\mu(\mathbf{q}) \neq \omega_\mu(2\mathbf{q})$.

From equation (26) we obtain that the second harmonic can be expressed as follows

$$u_\alpha^{(2)}(\mathbf{n},t) = \frac{1}{2}\sum_\nu \Big\{ e^{2i\mathbf{qn}} T_{\alpha\nu}(2\mathbf{q}) \frac{W_{\mu\mu\nu}(\mathbf{q},\mathbf{q},2\mathbf{q})}{\omega_\nu^2(2\mathbf{q}) - 4\omega_\mu^2(\mathbf{q})} \Phi_\mu^2(\mathbf{n},t) + e^{2i\mathbf{q'n}} T_{\alpha\nu}(2\mathbf{q'}) \frac{W_{\mu\mu\nu}(\mathbf{q'},\mathbf{q'},2\mathbf{q'})}{\omega_\nu^2(2\mathbf{q'}) - 4\omega_\mu^2(\mathbf{q'})} \Psi_\mu^2(\mathbf{n},t)$$
$$+2e^{i(\mathbf{q}+\mathbf{q'})\mathbf{n}} T_{\alpha\nu}(\mathbf{q}+\mathbf{q'}) \frac{W_{\mu\mu\nu}(\mathbf{q},\mathbf{q'},\mathbf{q}+\mathbf{q'})}{\omega_\nu^2(\mathbf{q}+\mathbf{q'}) - 4\omega_\mu^2(\mathbf{q})} \Phi_\mu(\mathbf{n},t)\Psi_\mu(\mathbf{n},t) \Big\} \quad (27)$$

where the notation

$$W_{\mu\nu\kappa}(\mathbf{k},\mathbf{k'},\mathbf{k''}) = 8i\sum_{\boldsymbol{\Delta}}\sum_{\alpha\beta\gamma} V_{\alpha\beta\gamma}(\boldsymbol{\Delta}) \sin(\frac{\mathbf{k}\boldsymbol{\Delta}}{2}) \sin(\frac{\mathbf{k'}\boldsymbol{\Delta}}{2}) \times \sin(\frac{\mathbf{k''}\boldsymbol{\Delta}}{2}) T_{\alpha\mu}(\mathbf{k}) T_{\beta\nu}(\mathbf{k'}) T_{\gamma\kappa}(\mathbf{k''}) \quad (28)$$

was introduced. It is seen from equations (21, 26) that the zeroth (quasistatic) harmonic in the expansion (19) consists of two parts

$$u_\alpha^{(0)}(\mathbf{n},t) = \zeta_\alpha(\mathbf{n},t) + \xi_\alpha(\mathbf{n},t). \quad (29)$$

The first term in this sum describes a spatially smooth quasistatic distribution. Its behavior is governed by the equation

$$\partial_t^2 \zeta_\alpha(\mathbf{n},t) = \sum_{\boldsymbol{\Delta},\beta} V_{\alpha\beta}(\boldsymbol{\Delta})(\zeta_\beta(\mathbf{n}-\boldsymbol{\Delta},t) - \zeta_\beta(\mathbf{n},t)) - 4i\sum_{\mathbf{kk'}}\sum_{\boldsymbol{\Delta},\beta,\gamma} V_{\alpha\beta\gamma}(\boldsymbol{\Delta}) \sin(\frac{(\mathbf{k}+\mathbf{k'})\boldsymbol{\Delta}}{2}) e^{i(\mathbf{k}+\mathbf{k'})\mathbf{n}} \times \Big\{ \sin^2(\frac{\mathbf{q}\boldsymbol{\Delta}}{2}) T_{\beta\mu}(\mathbf{q}) T_{\gamma\mu}(\mathbf{q}) \phi_\mu(\mathbf{k},t) \phi_\mu^*(-\mathbf{k'},t) + \sin^2(\frac{\mathbf{q'}\boldsymbol{\Delta}}{2}) T_{\beta\mu}(\mathbf{q'}) T_{\gamma\mu}(\mathbf{q'}) \psi_\mu(\mathbf{k},t) \psi_\mu^*(-\mathbf{k'},t) \Big\} \quad (30)$$

where $\phi_\mu(\mathbf{k},t)$ and $\psi_\mu(\mathbf{k},t)$ are the Fourier transforms of the amplitude functions defined in equation (22).The second term in equation (29) represents a spatially modulated quasistatic distribution. It can be written as follows

$$\xi_\alpha(\mathbf{n},t) = -\sum_\nu e^{i(\mathbf{q}-\mathbf{q'})\mathbf{n}} T_{\alpha\nu}(\mathbf{q}-\mathbf{q'}) \frac{W_{\mu\mu\nu}(\mathbf{q},\mathbf{q'},\mathbf{q}-\mathbf{q'})}{\omega_\nu^2(\mathbf{q}-\mathbf{q'})} \times \Psi_\mu^*(\mathbf{n},t)\Phi_\mu(\mathbf{n},t) + c.c. \quad (31)$$

In what follows we consider nonlinear excitations which are localized along the x-direction and modulated along the y-direction. This means that the amplitudes $\Phi_\mu(\mathbf{n},t)$ and $\Psi_\mu(\mathbf{n},t)$ are functions of n_x only. The Fourier components of the amplitudes $\Phi_\mu(\mathbf{n},t)$ and $\Psi_\mu(\mathbf{n},t)$ have the form

$$\phi_\mu(\mathbf{k}) = \bar{\phi}_\mu(k_x)\,\delta(k_y) \qquad \psi_\mu(\mathbf{k}) = \bar{\psi}_\mu(k_x)\,\delta(k_y). \quad (32)$$

Thus in the vicinity of the wave vectors (20) one can write

$$(\omega_\mu(\mathbf{q}+\mathbf{k}) - \omega_\mu(\mathbf{q}))\,\phi_\mu(\mathbf{k}) \simeq \left(v_\mu k_x + \frac{1}{2}\frac{\partial^2\omega_\mu(\mathbf{q})}{\partial q_x^2}k_x^2\right)\phi_\mu(\mathbf{k}) \quad (33)$$

and the same for $\psi_\mu(\mathbf{k})$. Here $v_\mu(\mathbf{q}) = \dfrac{\partial\omega_\mu(\mathbf{q})}{\partial q_x}$ is the excitation group velocity (note that $v_\mu(\mathbf{q}) = v_\mu(\mathbf{q'})$). We will consider excitations with group velocities v_μ less than the phase velocity of the mode μ in the x-direction $c_\mu = \lim_{k_x\to 0}\dfrac{\omega_\mu(k_x,q_y)}{k_x}$. Then in the reference frame moving with the group velocity v_μ when

$$\Phi_\mu(n_x,t) = \tilde{\Phi}_\mu(z,\tilde{t}) \qquad \Psi_\mu(n_x,t) = \tilde{\Psi}_\mu(z,\tilde{t}) \quad (34)$$

with $z = n_x - v_\mu t, \tilde{t} = t$, the smooth component $\zeta_\alpha(\mathbf{n}, t)$ can be considered as static and in the continuum limit it can be written as follows

$$\frac{\partial \zeta_\alpha(\mathbf{n},t)}{\partial n_x} = \frac{R_{\mu\alpha}(\mathbf{q})}{c_\alpha^2 - v_\mu^2}|\tilde{\Phi}_\mu(z,\tilde{t})|^2 + \frac{R_{\mu\alpha}(\mathbf{q}')}{c_\alpha^2 - v_\mu^2}|\tilde{\Psi}_\mu(z,\tilde{t})|^2 \quad (35)$$

where

$$R_{\mu\nu}(\mathbf{q}) = 4\sum_{\boldsymbol{\Delta}}\sum_{\alpha\,\beta} V_{\alpha\beta\nu}(\boldsymbol{\Delta}) \sin^2\left(\frac{\mathbf{q}\boldsymbol{\Delta}}{2}\right) \Delta_x T_{\alpha\mu}(\mathbf{q})\, T_{\beta\mu}(\mathbf{q}). \quad (36)$$

Inserting equations (27, 29, 31, 35) into equation (25) we obtain that the amplitudes of the excitations $\tilde{\Phi}_\mu(z,t)$ and $\tilde{\Psi}_\mu(z,t)$ satisfy the set of coupled nonlinear Schrödinger equations

$$\begin{aligned} -2i\omega_\mu(\mathbf{q})\frac{\partial}{\partial \tilde{t}}\tilde{\Phi}_\mu(z,\tilde{t}) &= \omega_\mu(\mathbf{q})\frac{\partial^2\omega_\mu(\mathbf{q})}{\partial q_x^2}\frac{\partial^2}{\partial z^2}\tilde{\Phi}_\mu(z,t) \quad (37)\\ &+B_{11}|\tilde{\Phi}_\mu(z,\tilde{t})|^2\,\tilde{\Phi}_\mu(z,\tilde{t}) + B_{12}|\tilde{\Psi}_\mu(z,\tilde{t})|^2\tilde{\Phi}_\mu(z,\tilde{t})\\ -2i\omega_\mu(\mathbf{q})\frac{\partial}{\partial \tilde{t}}\tilde{\Psi}_\mu(z,\tilde{t}) &= \omega_\mu(\mathbf{q})\frac{\partial^2\,\omega_\mu(\mathbf{q})}{\partial q_x^2}\frac{\partial^2}{\partial z^2}\tilde{\Psi}_\mu(z,\tilde{t})\\ &+B_{21}|\tilde{\Phi}_\mu(z,\tilde{t})|^2\,\tilde{\Psi}_\mu(z,\tilde{t}) + B_{22}|\tilde{\Psi}_\mu(z,\tilde{t})|^2\,\tilde{\Psi}_\mu(z,\tilde{t}). \end{aligned}$$

In the equations (37) the second derivatives $\partial_{\tilde{t}}^2\tilde{\Phi}, \partial_{\tilde{t}}^2\tilde{\Psi}$ and $\partial_z\partial_{\tilde{t}}\tilde{\Phi}, \partial_z\partial_{\tilde{t}}\tilde{\Psi}$ where omitted because, as mentioned above, the amplitudes $\tilde{\Phi}$ and $\tilde{\Psi}$ are slow functions of $\tilde{t}$ and z.

In equations (37) the following abbreviations were used

$$\begin{aligned} B_{11} &= \sum_\nu \left(\frac{|R_{\mu\nu}(\mathbf{q})|^2}{c_\nu^2 - v_\mu^2} + \frac{1}{2}\frac{|W_{\mu\mu\nu}(\mathbf{q},\mathbf{q},2\mathbf{q})|^2}{\omega_\nu^2(2\mathbf{q}) - 4\omega_\mu^2(\mathbf{q})}\right)\\ &\quad - 3W_{\mu\mu\mu\mu}(\mathbf{q},\mathbf{q},\mathbf{q},\mathbf{q}) \quad (38)\\ B_{22} &= idem\ (q \to q')\\ B_{12} = B_{21} &= \sum_\nu \left(\frac{R_{\mu\nu}(\mathbf{q})R_{\mu\nu}(\mathbf{q}')}{c_\nu^2 - v_\mu^2}\right.\\ &\quad \left. + \frac{|W_{\mu\mu\nu}(\mathbf{q},\mathbf{q}',\mathbf{q}-\mathbf{q}')|^2}{\omega_\nu^2(\mathbf{q}-\mathbf{q}')} + \frac{|W_{\mu\mu\nu}(\mathbf{q},\mathbf{q}',\mathbf{q}+\mathbf{q}')|^2}{\omega_\nu^2(\mathbf{q}+\mathbf{q}') - 4\omega_\mu^2(\mathbf{q})}\right)\\ &\quad - 6W_{\mu\mu\mu\mu}(\mathbf{q},\mathbf{q},\mathbf{q}',\mathbf{q}') \quad (39) \end{aligned}$$

with the notation

$$\begin{aligned} W_{\mu\nu\kappa\rho}(\mathbf{k},\mathbf{k}',\mathbf{k}'',\mathbf{k}''') &= 8\sum_{\boldsymbol{\Delta}\alpha,\beta,\gamma,\delta} V_{\alpha\beta\gamma\delta}(\boldsymbol{\Delta})\\ &\times \sin(\frac{\mathbf{k}\boldsymbol{\Delta}}{2})\sin(\frac{\mathbf{k}'\boldsymbol{\Delta}}{2})\sin(\frac{\mathbf{k}''\boldsymbol{\Delta}}{2})\sin(\frac{\mathbf{k}'''\boldsymbol{\Delta}}{2})\\ &\times T_{\alpha\mu}(\mathbf{k})T_{\beta\nu}(\mathbf{k}')T_{\gamma\kappa}(\mathbf{k}'')T_{\delta\rho}(\mathbf{k}'''). \quad (40) \end{aligned}$$

It is seen from equations (38, 28, 36, 40) that $B_{11} = B_{22}$.

It is convenient to change the time variable to $\tau = \frac{1}{2}\frac{\partial^2\omega_\mu(\mathbf{q})}{\partial q_x^2}t$ and rescale the amplitudes of the excitations to

$$\begin{aligned} A_\mu(z,\tau) &= \sqrt{\left|\frac{B_{11}}{\beta_\mu}\right|}\,\tilde{\Phi}_\mu(z,t),\\ B_\mu(z,\tau) &= \sqrt{\left|\frac{B_{11}}{\beta_\mu}\right|}\,\tilde{\Psi}_\mu(z,t) \quad (41)\\ \beta_\mu &= \omega_\mu\frac{\partial^2\omega_\mu(q_x)}{\partial q_x^2}\ . \end{aligned}$$

The function $A_\mu(z,\tau)$ and $B_\mu(z,\tau)$ satisfy the set of coupled equations

$$\begin{aligned} -i\frac{\partial}{\partial\tau}A_\mu(z,\tau) &= \frac{\partial^2}{\partial z^2}A_\mu(z,\tau) + s_\mu\ \left(|A_\mu(z,\tau)|^2\right.\\ &\quad \left.+\gamma_\mu|B_\mu(z,\tau)|^2\right)A_\mu(z,\tau)\\ -i\frac{\partial}{\partial\tau}B_\mu(z,\tau) &= \frac{\partial^2}{\partial z^2}B_\mu(z,\tau) + s_\mu\ \left(\gamma_\mu|A_\mu(z,\tau)|^2\right.\\ &\quad \left.+|B_\mu(z,\tau)|^2\right)B_\mu(z,\tau) \quad (42) \end{aligned}$$

where

$$s_\mu = \mathrm{sign}\left(\frac{B_{11}}{\beta_\mu}\right), \quad (43)$$

is Lighthill's parameter [17] and

$$\gamma_\mu = \frac{B_{12}}{B_{11}} \quad (44)$$

is the cross-phase modulation coefficient.

Thus the nonlinear energy transfer in anharmonic quadratic lattices is governed by a set of two nonlinearly coupled NLS equations which is one of the most generic models of nonlinear physics. Nonlinear coupling mechanisms occur in a large variety of wave phenomena and in particular in plasma physics, nonlinear optics and fluid dynamics. Examples are the propagation of transversal electro-magnetic waves in a cold plasma [18,19], the interaction between Langmuir and ion-acoustic waves [20], the light propagation in magneto-optically active media [21], the interaction between the surface wave packets in fluids [22], *etc.* The system (42) is not completely integrable. It has been shown [23] to be solvable by the inverse scattering transform only in the two cases:

i) $\gamma_\mu = 0$ (see Zakharov-Shabat [24]),
ii) $\gamma_\mu = 1, s_\mu = 1$ (see Manakov [25]).

In the general non-integrable case the system (42) was studied mostly numerically, but a few powerful approximate analytical methods were also proposed [26–31].

In the problem under consideration the nonlinear coupling takes place between the waves that belong to the star of the wave vector (20). When $\mathbf{q} = \mathbf{q}'$ ($q_y = 0$)

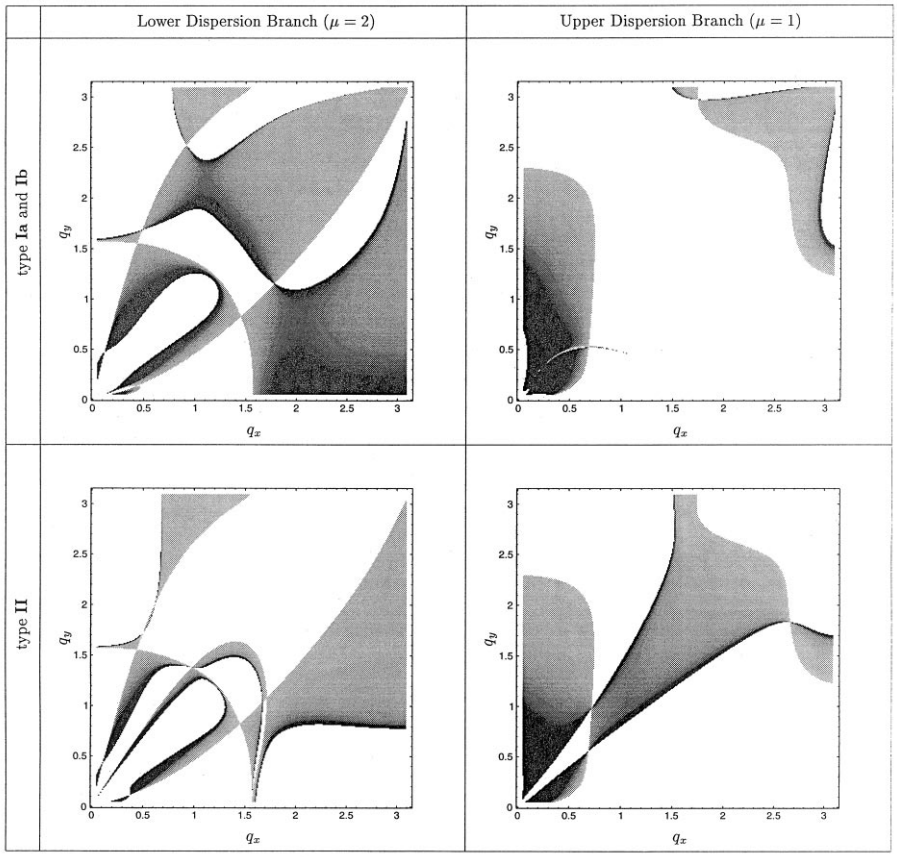

Fig. 1. These solution maps show the existence condition $s_\mu \Gamma_\mu > 0$ for envelope solitary waves in the NLS equation (47) for the types I and II under consideration and for each dispersion branch. We use the Morse potential (52) with $\alpha_1 = \alpha_{\sqrt{2}} = 0.1$ for the potential parameters. In the white areas $s_\mu \Gamma_\mu$ is less than zero, so no localized envelope solution can exist. In the shaded regions the blackness is proportional to the amplitude of the envelopes (for a fixed width). See the text for further discussion.

there is no modulation in the y-direction. It is seen from equations (14, 15, 36) that

$$\begin{aligned} T_{\alpha\mu}(\mathbf{q}) &= \delta_{\alpha\mu} \\ R_{\alpha\mu}(\mathbf{q}) &= \delta_{\alpha 1}\, R_{1\mu}(\mathbf{q}) \end{aligned} \quad \text{when} \quad q_y = 0. \tag{45}$$

Then we obtain from equations (23, 31, 35, 45) that the excitations with frequencies close to $\omega_1(q_x, q_y = 0)$ are pure longitudinal ($u_y(\mathbf{n}, t) \equiv 0$), while the excitations with frequencies near $\omega_2(q_x, q_y = 0)$ consist of an oscillatory transversal component $u_y(n_x, t)$ and a smooth longitudinal displacement $\zeta_x(n_x, t)$. In other words, we get the case which was studied in [15]. In the general case when $\mathbf{q} \neq \mathbf{q}'$, there is a modulation in the direction perpendicular to the movement of the excitation, and the structure of the excitations is much more complicated. One of the aims of the present paper is to study the effect of the modulation on the elastic energy transfer in two-dimensional lattices.

3 Solitary waves and their interactions

In the following we will examine two special solutions of (42) when the set of coupled NLS equations reduces to a single NLS equation. However, keeping in mind, that equations (42) are approximative solutions of the original discrete equations of motion (12) only, this is not a real restriction. The decoupling condition, which we will consider in the following, is valid in the continuum approximation only, doesn't imply that the description of the discrete model is restricted by any means. The only reason, why this way was chosen, is the considerable simplification of the following analytical treatment.

Hence, we confine ourselves here to an investigation of two types of solutions

$$\begin{aligned} I_a: &\quad A \neq 0,\ B = 0 \\ I_b: &\quad A = 0,\ B \neq 0 \\ II: &\quad A = B. \end{aligned} \tag{46}$$

In all these cases the system (42) reduces to the NLS equation of the form

$$-i\frac{\partial}{\partial \tau} F_\mu(z,\tau) = \frac{\partial^2}{\partial z^2} F_\mu(z,\tau) + s_\mu\, \Gamma_\mu |F_\mu(z,\tau)|^2\, F_\mu(z,\tau) \tag{47}$$

where $\Gamma_\mu = 1$ for the first type solutions and $\Gamma_\mu = 1 + \gamma_\mu$ for the second type solutions. Equation (47) has localized solutions only when $s_\mu \Gamma_\mu > 0$. The dependence

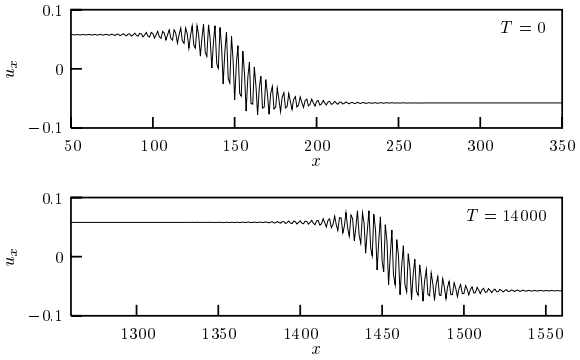

Fig. 2. Profile plot of the longitudinal displacement u_x for a type-I_a excitation for time $T = 0$ and time $T = 14\,000$. We used a wave vector $\mathbf{q} = (1.8, 1.05)$ and an inverse width of $\epsilon = 1/L = 0.06$. Note that there is practically no radiation.

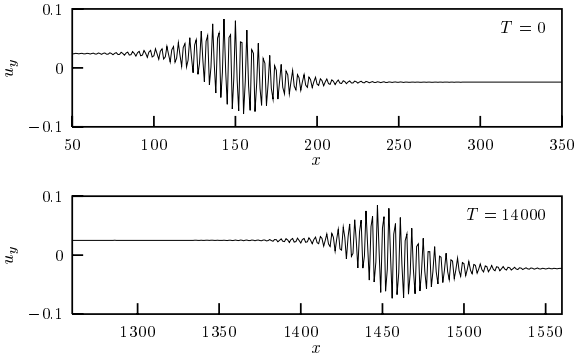

Fig. 3. Profile plot of the traversal displacements u_y of a type-I_a excitation for time $T = 0$ and time $T = 14\,000$. Same parameters as in Figure 2.

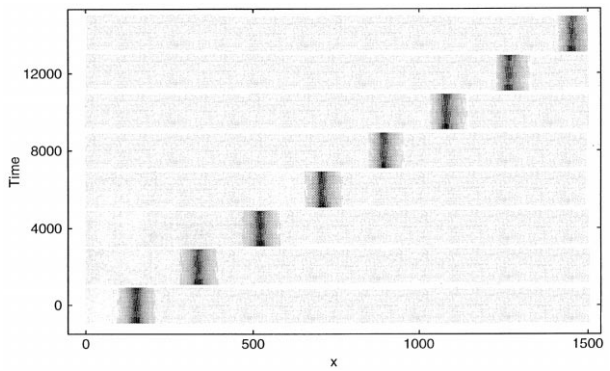

Fig. 4. Energy density plot for the type-I_a excitation from Figures 2 and 3. Every stripe corresponds to a snapshot of the lattice where one period of the modulation along the transversal directions is plotted.

of the function $s_\mu \Gamma_\mu$ on the carrier wave vector $\mathbf{q}$ for a specific potential is shown in Figure 1. Here we show a plot for each dispersion branch ($\mu = 1, 2$) and solution type. In the white areas $s_\mu \Gamma_\mu$ is negative and there are no localized solutions. The brightness in dark areas characterizes the value of $\dfrac{\beta_\mu}{\Gamma_\mu B_{11}}$: the darker the point, the bigger is this quantity. Taking into account that the solitary-wave

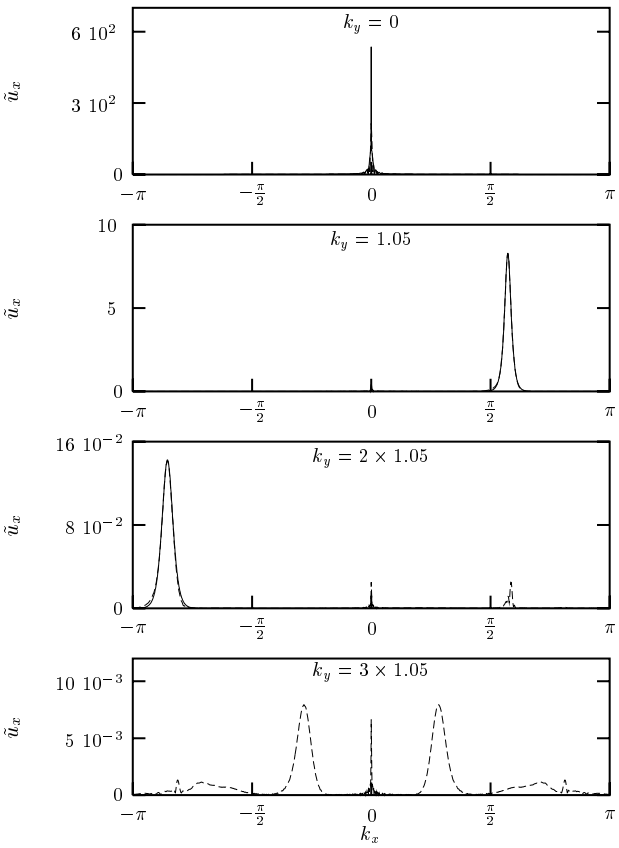

Fig. 5. Space Fourier spectrum of the longitudinal displacements of the type-I_a solitary waves in Figure 2. The solid lines represent the initial spectrum whereas the dashed lines show the spectrum at time $T = 14\,000$. We show different plots for each harmonic of the transversal modulation (the plot with $k_y = 0$ corresponds to the kink part of the solitary waves). One can see clearly that the shapes of the Fourier transforms are well preserved over time. Note also the different scales of the amplitudes, which differ at least one order of magnitude between two successive harmonics. The initially not excited third harmonic remains very small which confirms our assumption in equations (24–26).

solution to the equation (47) has the form

$$F_\mu(z,\tau) = \epsilon\sqrt{\frac{2}{s_\mu \Gamma_\mu}}\, e^{-i\frac{C}{2}z + i(\epsilon^2 - \frac{C^2}{4})\tau}\,\mathrm{sech}(\epsilon(z + C\tau)) \tag{48}$$

where C is the velocity in the moving frame of reference and ϵ is the inverse width of the excitation, one obtains that the amplitudes Φ_μ and Ψ_μ are proportional to $\dfrac{\beta_\mu}{\Gamma_\mu B_{11}}$ according to equation (41). So one can also say that at fixed width the amplitude of the Φ_μ-solitary wave (or Ψ_μ-solitary wave) is larger in dark regions than in light ones. We also see that moving along the q_y axis for fixed q_x one can be either in a dark area or in a light one. To put it in another way, the solitary-wave solutions may or may not exist depending on the modulation wave number q_y.

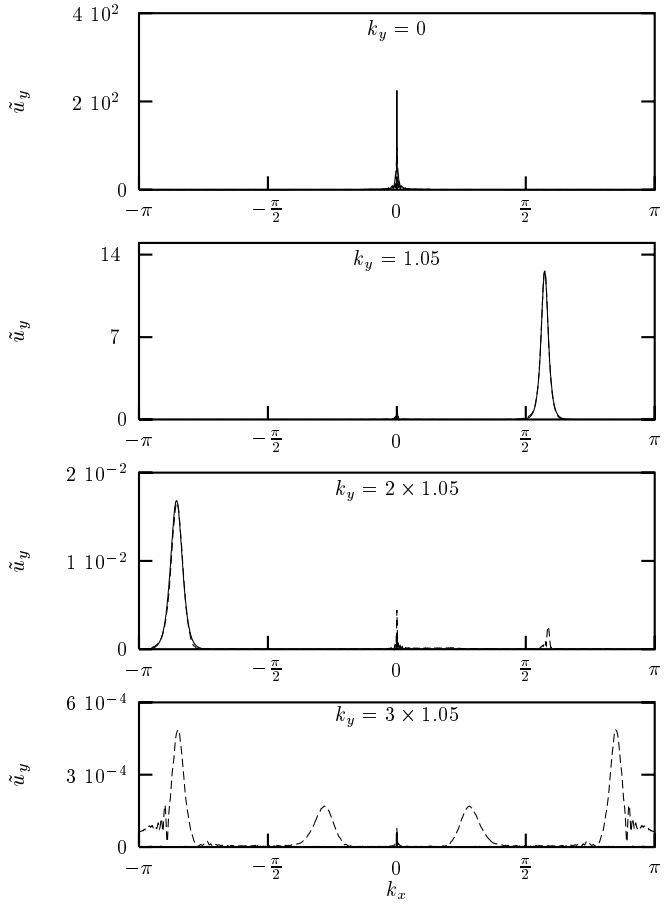

Fig. 6. Space Fourier transform of the transversal displacements of the type-I_a excitation in Figure 3.

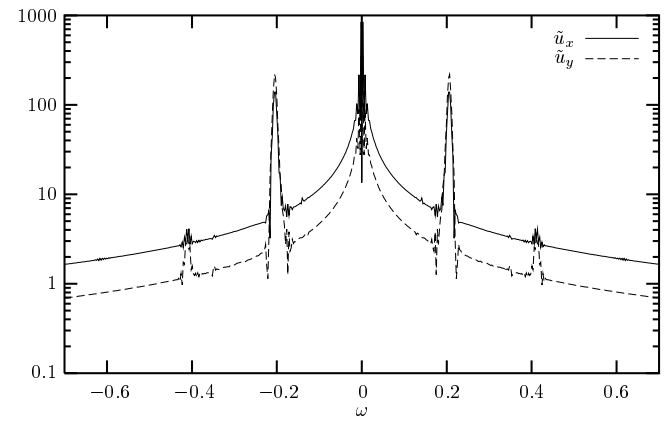

Fig. 7. Time Fourier Spectrum for the type-I_a excitation from Figure 2 and 3. The plot shows the time Fourier transforms $\tilde{u}_x$ and $\tilde{u}_y$ of point $\mathbf{n} = (1380, 2)$ between the times $T = 12\,000$ and $T = 14\,400$. The harmonic frequency in this case is $\omega_2 = 0.21$. Note the logarithmic scale for $\tilde{u}_x$ and $\tilde{u}_y$.

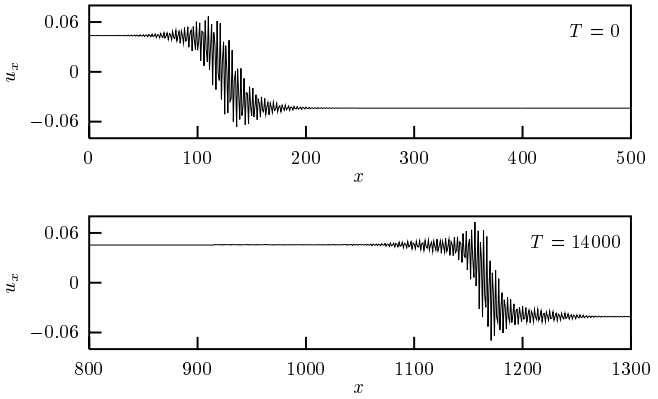

Fig. 8. Profile plot for u_x of a type-II excitation for time $T = 0$ and time $T = 14000$. Here we used a wave vector $\mathbf{q} = (2.3, 1.05)$ and an inverse width of $\epsilon = 1/L = 0.06$.

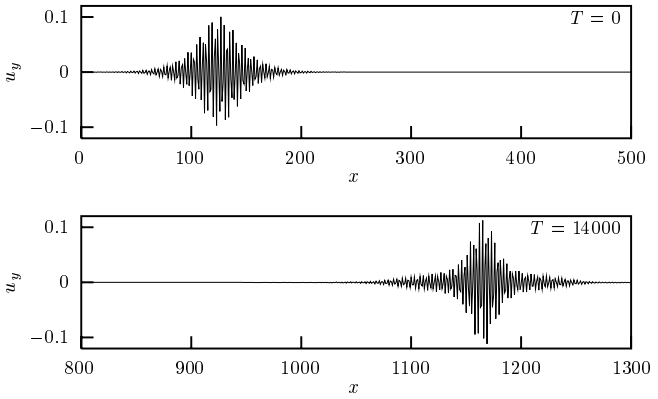

Fig. 9. Profile plot for u_y of a type-II excitation for time $T = 0$ and time $T = 14\,000$. Same parameters as in Figure 8.

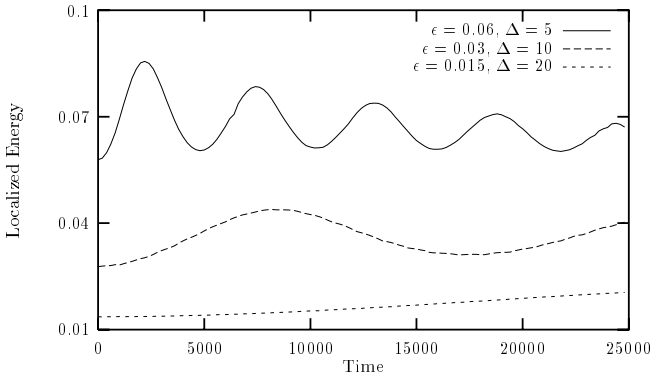

Fig. 10. The energy which is localized around the center of solitary waves of type-II *versus* time. The carrier wave vector is $\mathbf{q} = (2.3, 1.05)$, ϵ is the amplitude parameter defined in equation (48) and Δ is the length of the interval along the x-axis in which the energy is measured. The localized energy is inversely proportional to the width of the solitary waves. The frequency of the oscillations of the width is approximately proportional to the square of the amplitudes.

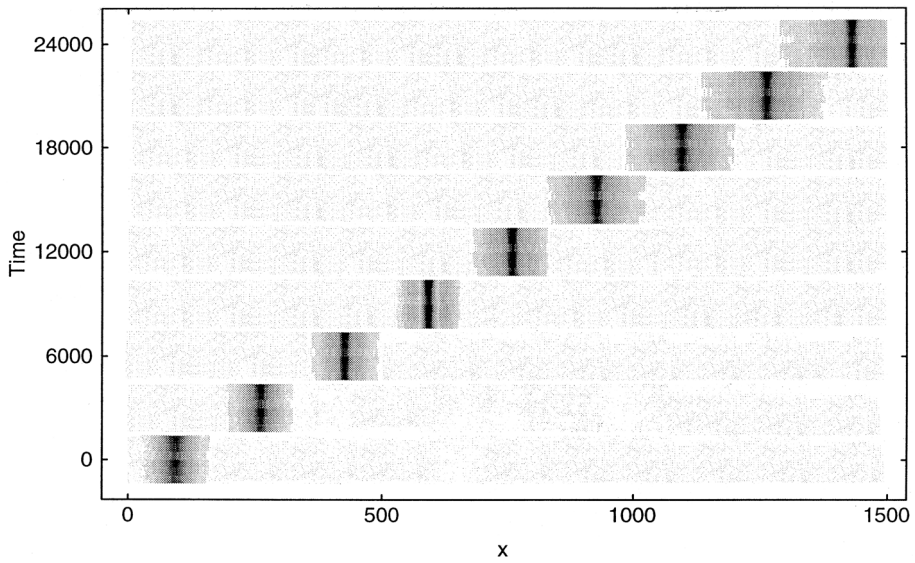

Fig. 11. Energy density plot for the type-II excitation from Figure 8. Same kink of plot as in Figure 4.

We consider solitary waves which propagate with a velocity equal to the group velocity $v_\mu(\mathbf{q})$ (this means that we set $C = 0$ in equation (48)). In this case we obtain from (19, 23, 27, 29, 31, 41, 48) that the atomic displacements $u_\alpha(\mathbf{n}, t)$ may be written as follows

$$\mathrm{I_a)}\ u_\alpha(\mathbf{n},t) = 2\epsilon \left|\frac{\beta_\mu}{B_{11}}\right| \frac{R_{\mu\alpha}(\mathbf{q})}{c_\alpha^2 - v_\mu^2(\mathbf{q})} \tanh(\epsilon(n_x - v_\mu(\mathbf{q})t)) \tag{49}$$

$$+ 2\epsilon\sqrt{2\left|\frac{\beta_\mu}{B_{11}}\right|}\, T_{\alpha\mu}(\mathbf{q}) \cos(\mathbf{qn} - (\omega_\mu(\mathbf{q}) - \frac{\epsilon^2}{2}\frac{\beta_\mu}{\omega_\mu(\mathbf{q})})t)$$

$$\times \operatorname{sech}(\epsilon(n_x - v_\mu(\mathbf{q})t)) + \mathcal{O}(\epsilon^2)$$

$$\mathrm{I_b)}\ \textit{idem}\ (\mathbf{q} \to \mathbf{q}') \tag{50}$$

$$\mathrm{II)}\ u_\alpha(\mathbf{n},t) = \tag{51}$$

$$2\epsilon \left|\frac{\beta_\mu}{B_{11}+B_{12}}\right| \frac{R_{\mu\alpha}(\mathbf{q}) + R_{\mu\alpha}(\mathbf{q}')}{c_\alpha^2 - v_\mu^2(\mathbf{q})} \tanh(\epsilon(n_x - v_\mu(\mathbf{q})t))$$

$$+ 4\epsilon\sqrt{2\left|\frac{\beta_\mu}{B_{11}+B_{12}}\right|}\, T_{\alpha\mu}(\mathbf{q})\, \cos(q_y\, n_y + \frac{\alpha-\mu}{2}\,\pi)$$

$$\times \cos(q_x\, n_x - (\omega_\mu(\mathbf{q}) - \frac{\epsilon^2}{2}\frac{\beta_\mu}{\omega_\mu(\mathbf{q})})t - \frac{\alpha-\mu}{2}\,\pi)$$

$$\times \operatorname{sech}(\epsilon(n_x - v_\mu(\mathbf{q})t)) + \mathcal{O}(\epsilon^2).$$

For the sake of simplicity we omitted the terms of order ϵ^2. Note however, that we included for the numerical simulations, beside the expressions (49, 50), also the second order terms given by (23, 27, 31) in the initial conditions. These terms are important, because only in this case we could avoid the creation of additional kinks and ripples.

The solutions given by equations (49, 50) are a superposition of a kink and a symmetric envelope solitary wave, both moving with velocity $v_\mu(\mathbf{q})$ in the x-direction. It is seen from equations (49, 50) that in the case I the envelope solitary wave is a linearly polarized wave, while in the case II it is a wave with elliptic polarization. The carrier wave of the type-I envelope solitary wave propagates with its phase velocity in a direction which depends on the carrier wave vector $\mathbf{q}$ ($\mathbf{q}'$). In the case II the carrier wave is a combination of a propagating longitudinal wave and a standing transversal wave. The kinks in the solution (49–50) are either rarefactive or compressive, according to the sign of $\dfrac{R_{\mu\alpha}(\mathbf{q})}{c_\alpha^2 - v_\mu^2(\mathbf{q})}$. In the case II the kink in the transversal displacements ($\alpha = 2$) vanishes because $R_{\mu 2}(\mathbf{q}) = -R_{\mu 2}(\mathbf{q}')$ (see Eq. (36)) and $u_y(\mathbf{n}, t)$ becomes symmetric in $\mathbf{n}$.

To check the stability and long-time behavior of the solitary-wave solutions obtained from the NLS equations (37), we performed molecular dynamics computer simulations. We used an interatomic Morse potential

$$V_\Delta(x) = \left(1 - e^{-\alpha_\Delta(x-\Delta)}\right)^2 \tag{52}$$

with $\alpha_1 = \alpha_{\sqrt{2}} = 0.1$ as potential parameters for NN and NNN interactions, respectively. Note that, in addition to the Taylor expansions (6, 8, 10) we also performed simulations for the full potential (52) as reference. A comparison of those simulations showed, that the Taylor expanded potentials and the simulations of the full Morse potential yield the same results within 0.5% difference in the displacements, which confirms the accuracy of the expanded potentials.

We used periodic boundary conditions for the (transversal) y-direction and free boundaries along the (longitudinal) x-direction. The equations of motion were integrated using a symplectic solver [32] and, for comparison, a fourth order Runge-Kutta scheme. The time step was fixed so that the total energy was conserved up to a relative error of 10^{-4}. The length of the lattice in x-direction was chosen between 500 and 1000 particles depending on the width and velocity of the excitations and

the duration of the simulation. The width of the lattice in y-direction was chosen in such a way that exactly one period of the applied transversal modulation fitted into the lattice. We also used larger lattice widths with more modulation periods included and checked that modes with longer wavelengths were not excited.

In Figures 2 and 3 we present the longitudinal and transversal components of the atomic displacements for the type-I_a solitary wave in a chain with Morse interatomic interactions (52), a carrier wave vector $\mathbf{q} = (1.8, 1.05)$ and the frequency which corresponds to the lower branch $\mu = 2$. As initial condition we used equation (49) with $\epsilon = 0.06$. The solitary wave is moving with velocity 0.09. The kink parts for both the longitudinal and transversal component are rarefactive. The solitary wave is very stable and there is practically no radiation. Figure 4 shows the time evolution of the energy density. The solitary wave has a complicated internal structure. To check how the structure changes in time we calculated the Fourier-transform of the initial condition (49) and of the evolved solitary wave at time $T = 14\,000$. The results are presented in Figures 5–7. It is seen that in the course of the experiment the internal structure of the solitary wave practically does not change.

For type-II excitations the situation is more complicated. Figures 8 and 9 show the initial condition and a snapshot at time $T = 14\,000$ for a type-II excitation with $\mathbf{q} = (2.3, 1.05)$ and $\mu = 2$. In contrast to the previously discussed type-Ia solutions there is an additional dynamical behaviour: the width of the excitations oscillates with an amplitude dependent frequency. This can be seen very clearly in Figure 10, where we plotted the energy localized in a certain fixed interval around the center of mass versus time for different solitary wave amplitudes. A maximum in the curve indicates a minimal width of the solitary wave. Figure 11 shows an energy density plot for a type-II excitation and gives a direct impression of the reshaping behaviour. We remind that for the dynamics of type-II excitations both amplitudes contribute to the coupled NLS equations (37). This situation is similar to the case of an optical fiber supporting two distinct propagating modes [26], where the system is also governed by two coupled NLS equations. Direct numerical simulations of this set of equations [33–36] produce the same behaviour as our type-II excitations, namely the reshaping of the envelopes in course of the time. Ueda and Kath examined this behaviour analytically using a collective variable approach [26] and estimated for the frequency of the width oscillation:

$$\omega_i = \frac{32}{\pi} \frac{\beta_\mu^2}{B_{11} + B_{12}} \epsilon^2 \quad . \tag{53}$$

Inserting the parameters from the simulations of Figures 8 and 9 we obtain a period $T_i \approx 36\,000$ for $\epsilon = 0.03$ which is within the same order of magnitude as the oscillations in Figure 10 ($T_i \approx 18\,000$). Furthermore the quadratic dependence on the amplitude is also confirmed approximately. We conclude that the reshaping of the solitary waves of the coupled NLS equations found previously in nonlinear optics and the reshaping found in the simulations of our discrete system have presumably the same origin.

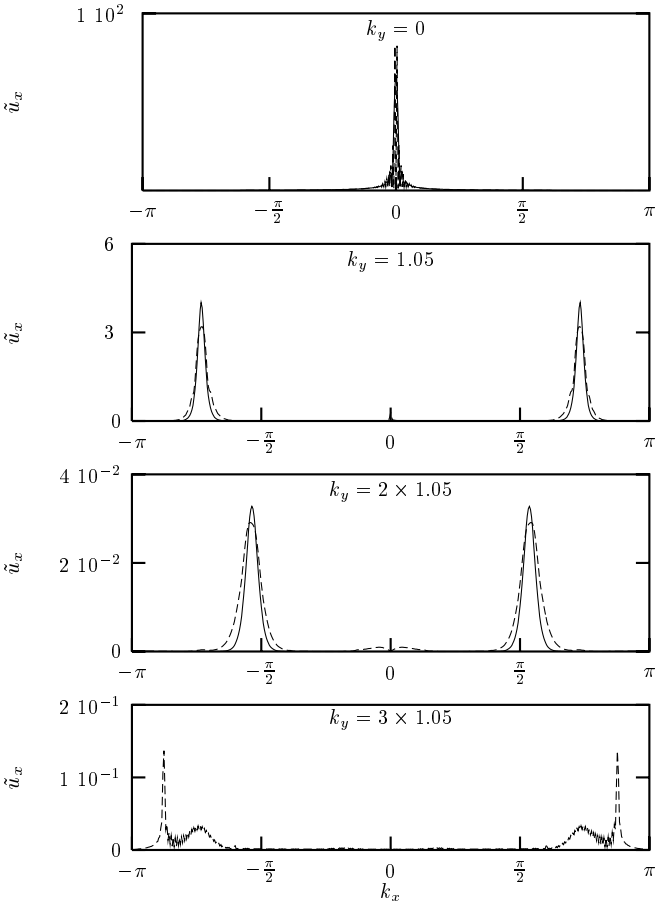

Fig. 12. Space Fourier spectrum of the longitudinal displacements of the type-II excitation in Figure 8. The solid lines represent the initial excitations whereas the dashed lines show the spectrum at time $T = 14\,000$. We show different plots for each harmonic of the transversal modulation. One can see that the third harmonic for the modulation in transversal direction is considerably excited and contributes significantly to the excitation.

The Fourier plots in Figures 12 and 13 give also evidence that type-II solitary waves are not fully described by the solutions (50). Note that the third harmonic in the longitudinal displacement is considerably excited, which makes our approximation in equations (24–26) invalid for this particular case.

In Figures 15 and 16 we present a collision between two type-I_a solitary waves moving in opposite directions (their carrier wave vectors are $\mathbf{q} = (2, 2.09)$ and $\mathbf{q} = -(2, 2.09)$). The solitary waves preserve their shape under the collision and there is negligible remanent radiation.

In Figures 17 and 18 we present a collision between type-I_a and type-I_b solitary waves. In contrast to the previous case the scattering is apparently non-elastic. During the collision the two solitary waves pass through each other but some radiation is shedded. Such a difference between scattering of solitary waves of the same type and

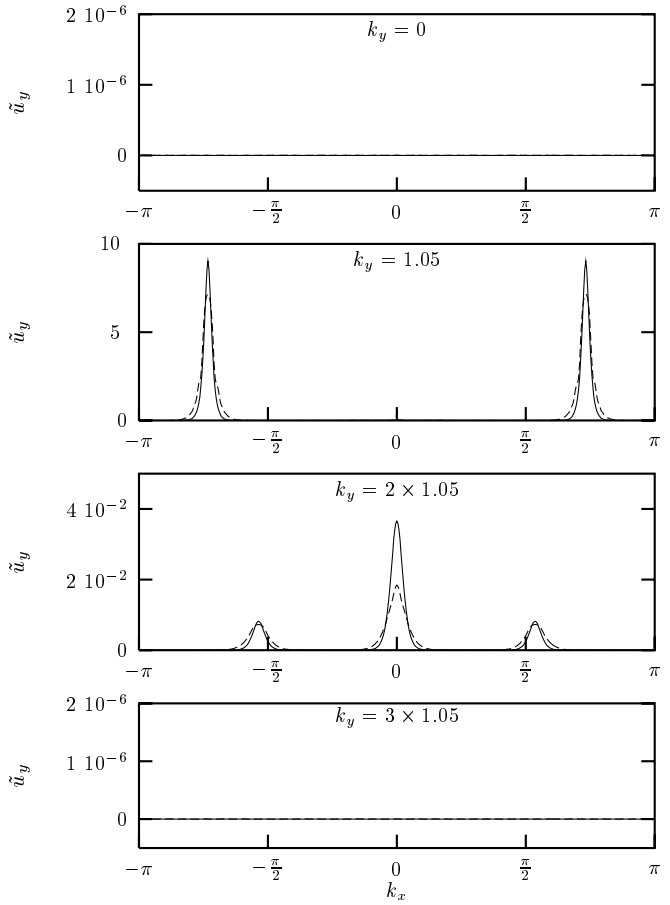

Fig. 13. Space Fourier transform of the transversal displacements of the type-II excitation in Figure 9. The solid lines corresponds to $T = 0$, the dashed lines represent the spectrum at $T = 14\,000$.

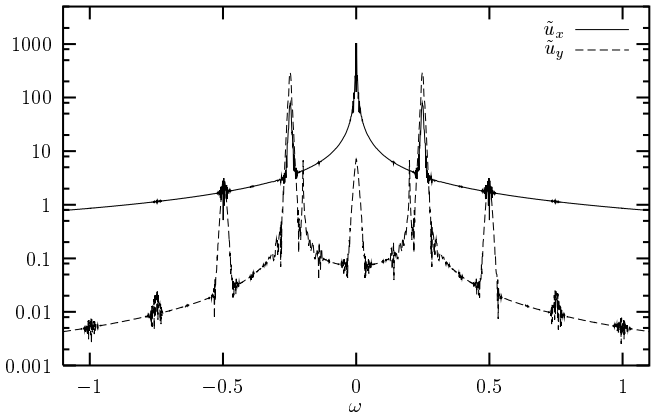

Fig. 14. Time Fourier Spectrum of the type-II excitation in Figures 8 and 9. The plot shows the time Fourier transforms of the longitudinal and transversal displacements of point $\mathbf{n} = (1215, 2)$ between the times $T = 12\,400$ and $T = 16\,400$. Due to the absence of a non-oscillating contribution to the transversal displacement in order $\mathcal{O}(\epsilon^1)$ one can see nicely the higher harmonics which were excited though they remain quite small. Note the logarithmic scale for $\tilde{u}_x$ and $\tilde{u}_y$.

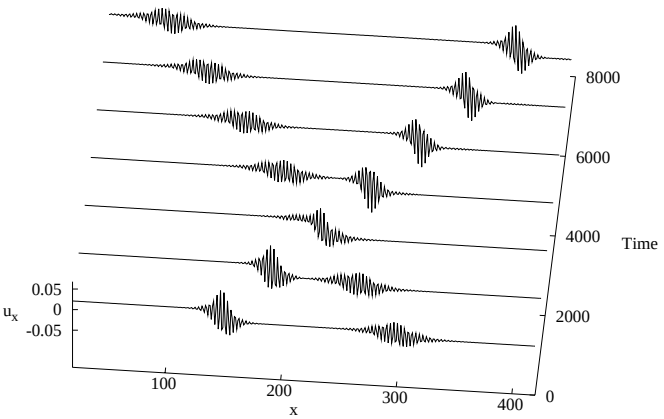

Fig. 15. Time evolution for the scattering of two type-I_a solitary waves which have carrier wave vectors of $\mathbf{q} = (2.0, 1.05)$ and $\mathbf{q} = (-2.0, -1.05)$. The inverse width of the bigger structure is $\epsilon = 1/L = 0.16$, for the small structure $\epsilon = 0.08$. Only the longitudinals displacement displacements u_x are shown.

of different types is not unexpected. Indeed, the dynamics of the collision between two type-I_a (or I_b) waves is governed mainly by the first NLS equation in (42), while the component $B(z,t)$ plays the role of a small perturbation. The almost elastic collision of solitary waves in this case is the result of the integrability of the NLS equation. However, when two solitary waves of different types interact, the dynamics is governed by a system of coupled NLS equations which is nonintegrable. The scattering of two solitary of different types in the framework of the system of two coupled NLS equations was studied in [31]. It was shown that the collisions are essentially nonelastic. During collision some radiation is shedded and daughter solitary waves are generated [31]. Taking into account that the system (42) represents only an approximate description of the lattice dynamics, it is evident that in this case the nonelastic nature of the soliton-soliton scattering in this case should be more pronounced than in [31].

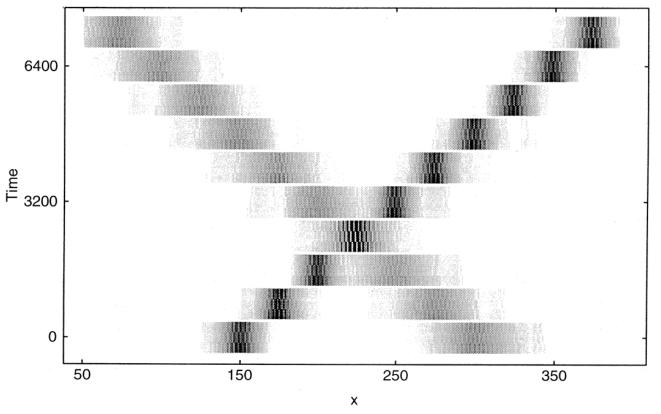

Fig. 16. Energy density plot for the scattering of the two type-I_a excitations from Figure 15.

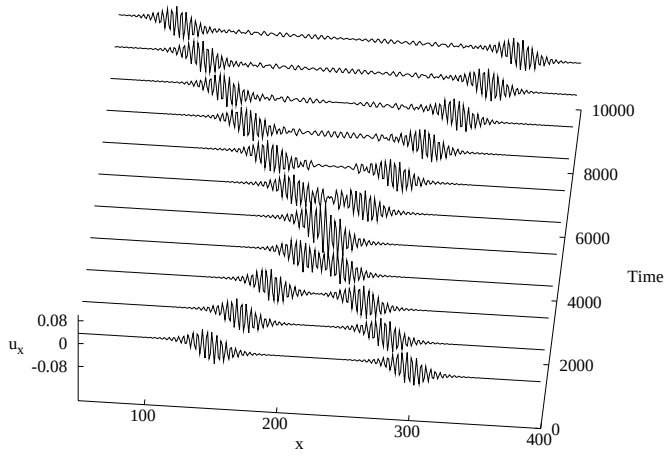

Fig. 17. Time evolution for a scattering experiment with a type-I_a and a type-I_b excitation. The parameters are $\mathbf{q} = (1.75, 1.05)$, $\epsilon = 0.1$ for the type-I_a excitation on the left and $\mathbf{q}' = (-1.75, 1.05)$, $\epsilon = 0.1$ for the type-I_b excitation on the right. Only the longitudinal displacements are shown.

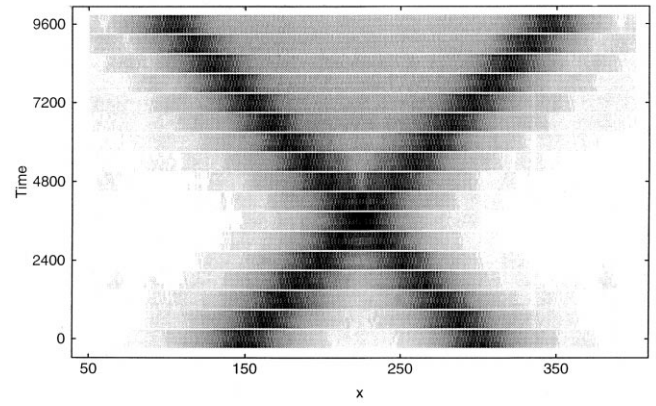

Fig. 18. Energy density plot for the scattering experiment of Figure 17.

4 Conclusions

We have examined the nonlinear dynamics of anharmonic two-dimensional square lattices with anharmonic interactions of third and fourth order taking into account the vector character of the atomic displacements. We have shown that in the quasi-monochromatic approximation and low-amplitude limit the dynamics of the two-dimensional square lattice is governed by a system of two coupled nonlinear Schrödinger equations for two slowly varying envelope amplitudes. The two amplitudes come here into existence as a consequence of the symmetry of the lattice: in general, there are two nonequivalent wave vectors in the first Brillouin zone for which the frequencies and group velocities of linear eigenmodes coincide.

The conditions for the existence of spatially localized nonlinear excitations and their dependence on the modulation wave vector were examined with the help of solution maps. It was shown that the nonlinear excitations are a superposition of a kink and an envelope solitary wave. The kink is either rarefactive or contractive depending on the parameters of the problem. We considered two types of excitations: linearly and elliptically polarized envelope solitary wave. For type-I the envelope solitary wave are accompanied by kinks in both the longitudinal and transversal displacements. The elliptically polarized envelope solitary wave (type-II) are symmetric in the transversal displacements (there is no kink component) and asymmetric for the longitudinal displacements.

Our analytical solitary wave solutions were tested by longtime molecular dynamics computer simulations. The type-I solitary waves completely preserve their shapes, also in collision experiments. For the type-II solitary waves we observe a reshaping, namely oscillations of the width. This behaviour is compared to analytical and numerical results obtained from coupled NLS equations in nonlinear optics. We conclude that the reshaping presumably has the same origin in both systems. In the scattering between type-I_a and type-I_b solitary waves a small part of the energy is converted into radiation of linear excitations.

Yu. Gaididei would like to express his thanks for the hospitality of the University of Bayreuth where this work was done. Partial support was received from project X 271.5 of the scientific and technological cooperation between Germany and Ukraine.

Appendix: Multiple scale analysis

It turned out that the simulations presented in Section 3 are fairly sensitive to the "right" choice of initial conditions, *i.e.* our analytical solutions have to be very close to the solutions of the discrete system.

The main assumption of the following analysis is the separation of the dynamics of the particle displacements on different time and space scales. This is a generalization of the idea of envelope solitary waves for which the smooth envelope is treated separately from the strongly oscillating carrier wave (*e.g.* see [6]). The hierarchy of scales is taken into account by introducing a new set of independent variables

$$\begin{aligned} \mathbf{n}_i &= \epsilon^i \mathbf{n} \\ t_i &= \epsilon^i t \ , \end{aligned} \tag{54}$$

where ϵ is the small parameter separating the scales. Furthermore we expand the displacement in the following way:

$$u_\alpha(\mathbf{n}) = \sum_{l=1}^{\infty} \epsilon^l u_{l,\alpha}\left(\mathbf{n}_0, \{\mathbf{n}_i\}; t_0, \{t_i\}\right). \tag{55}$$

Here $\alpha \in \{x, y\}$ designates the longitudinal (x) and transversal (y) directions and $\{\mathbf{n}_i\}$ and $\{t_i\}$ ($i \geq 1$) symbolize the set of slow space and time variables.

In the next step we expand the relative displacements (11) between two neighboring particles in a Taylor

series with respect to $\epsilon\boldsymbol{\Delta}$ on the slow scales:

$$\begin{aligned}
&u_\alpha(\mathbf{n}_0-\boldsymbol{\Delta},\{\mathbf{n}_i-\epsilon^i\boldsymbol{\Delta}\})-u_\alpha(\mathbf{n}_0,\{\mathbf{n}_i\})=\\
&u_\alpha(\mathbf{n}_0-\Delta,\{\mathbf{n}_i\})-u_\alpha(\mathbf{n}_0,\{\mathbf{n}_i\})\\
&-\sum_{l\beta}\epsilon^l\frac{\partial}{\partial n_{l,\beta}}u_\alpha(\mathbf{n}_0-\boldsymbol{\Delta},\{\mathbf{n}_i\})\Delta_\beta\\
&+\frac{1}{2}\sum_{lm\beta\gamma}\epsilon^{l+m}\frac{\partial}{\partial n_{l,\beta}}\frac{\partial}{\partial n_{m,\gamma}}u_\alpha(\mathbf{n}_0-\boldsymbol{\Delta},\{\mathbf{n}_i\})\Delta_\beta\Delta_\gamma\\
&+\ \ldots\ldots
\end{aligned}\tag{56}$$

Inserting this expression into the equations of motion (12) and considering separately each order in ϵ we obtain in $\mathcal{O}(\epsilon^1)$ the linear equation

$$\begin{aligned}
&\partial_{t_0t_0}u_{1,\alpha}(\mathbf{n}_0,t_0,\ldots)=\\
&\qquad\sum_{\boldsymbol{\Delta}\beta}V_{\alpha\beta}(\Delta)\left[u_{1,\beta}(\mathbf{n}_0-\boldsymbol{\Delta},t_0,\ldots)-u_{1,\beta}(\mathbf{n}_0,t_0,\ldots)\right].
\end{aligned}\tag{57}$$

Unfortunately this means that the calculations become very complex, *e.g.*, see equation (38). In order to eliminate all errors it proved to be advantageous to use two different ways of analytical treatment. In this section we apply a *Multiple Scale Analysis* to the equations of motion (12), generalizing Konotop's treatment of the one-dimensional case [37]. As we shall see, the approach used in Section 2 and the multiple scale calculations presented here lead to exactly the same results.

Here and in the following we indicate only the dependency on the fastest variables to enhance lucidity.

The general solution to this equation is obviously a superposition of the linear eigenmodes $T_{\alpha\mu}$ defined in (14) on the fastest scale. But in contrast to [37] we should also include a smooth component $D_{\mu'}$ which does not depend on the fast variables $\mathbf{n}_0$ and t_0 on the same footing as the principal envelope structure. As in Section 2 we consider the star of a fixed carrier wave vector $\mathbf{q}$ and one dispersion branch μ with harmonic frequency ω_μ, so the general solution reads

$$\begin{aligned}
u_{1,\alpha}(\mathbf{n}_0,t_0,\ldots)=\ &e^{-i(\omega_\mu t_0-\mathbf{q}\mathbf{n}_0)}T_{\alpha\mu}(\mathbf{q})\ \Phi_\mu(x_1,t_1,\ldots)\\
&e^{-i(\omega_\mu t_0-\mathbf{q}'\mathbf{n}_0)}T_{\alpha\mu}(\mathbf{q}')\ \Psi_\mu(x_1,t_1,\ldots)\\
&+\sum_{\mu'}T_{\alpha\mu'}(0)\ D_{\mu'}(x_1,t_1,\ldots)+c.c.
\end{aligned}\tag{58}$$

with $\mathbf{q}=(q_x,q_y)$ and $\mathbf{q}'=(q_x,-q_y)$. Similar to equation (32) we consider only nonlinear excitations which are localized in x-direction and periodically modulated along the y-direction and hence drop the space dependency on $\{y_i\}$ for Φ_μ, Ψ_μ and D_μ.

In the next-higher order $\mathcal{O}(\epsilon^2)$ we obtain the equation

$$\begin{aligned}
&\partial_{t_0t_0}u_{2,\alpha}(\mathbf{n}_0,t_0,\ldots)-\sum_{\boldsymbol{\Delta}\beta}V_{\alpha\beta}(\Delta)(u_{2,\beta}(\mathbf{n}_0-\boldsymbol{\Delta},t_0,\ldots)\\
&-u_{2,\beta}(\mathbf{n}_0,t_0,\ldots))=-2\partial_{t_0t_1}u_{1,\alpha}(\mathbf{n}_0,t_0,\ldots)\\
&-\sum_{\boldsymbol{\Delta}\beta}V_{\alpha\beta}(\Delta)\Delta_x\partial_{x_1}u_{1,\beta}(\mathbf{n}_0-\boldsymbol{\Delta},t_0,\ldots)\\
&+\sum_{\Delta\beta\gamma}V_{\alpha\beta\gamma}(\Delta)\big[(u_{1,\beta}(\mathbf{n}_0-\boldsymbol{\Delta},t_0,\ldots)-u_{1,\beta}(\mathbf{n}_0,t_0,\ldots))\\
&\times(u_{1,\gamma}(\mathbf{n}_0-\boldsymbol{\Delta},t_0,\ldots)-u_{1,\gamma}(\mathbf{n}_0,t_0,\ldots))\Big].
\end{aligned}\tag{68}$$

To fulfill this equation we must take into account the second harmonic as well as an additional smooth contribution in the displacement $\mathbf{u}_2$:

$$\begin{aligned}
u_{2,\alpha}(\mathbf{n}_0,t_0,\ldots)=\sum_{\mathbf{k}'\mu'}\Big[\ &\tilde{D}^{\mu'}_{\mathbf{k}'}(x_1,t_1,\ldots)\\
&+B^{\mu'}_{\mathbf{k}'}(x_1,t_1,\ldots)\,e^{-i\omega_\mu t_0}\\
&+B^{\mu'(2)}_{\mathbf{k}'}(x_1,t_1,\ldots)\,e^{-2i\omega_\mu t_0}\ \Big]\\
&\times e^{i\mathbf{k}'\mathbf{n}_0}T_{\alpha\mu'}(\mathbf{k}')+c.c.
\end{aligned}\tag{69}$$

Substituting (69) in (68) and using the orthogonality and completeness properties of the linear eigenmodes $T_{\alpha\mu'}$ we single out one equation for each harmonic (see also [37]). For the non-oscillating component we obtain

$$\begin{aligned}
\tilde{D}^{\mu'}_{\mathbf{k}'}(x_1,t_1,\ldots)=&-\frac{W_{\mu\mu\mu'}(\mathbf{q},\mathbf{q}',\mathbf{q}-\mathbf{q}')}{\omega^2_{\mu'}(\mathbf{q}-\mathbf{q}')}\ \delta_{\mathbf{k}',\mathbf{q}-\mathbf{q}'}\\
&\times\Phi_\mu(x_1,t_1,\ldots)\Psi^*_\mu(x_1,t_1,\ldots).
\end{aligned}\tag{70}$$

The terms proportional to the first harmonic $e^{-i\omega_\mu t_0}$ yield

$$\begin{aligned}
2i\omega_\mu\partial_{t_1}\Phi_\mu(x_1,t_1,\ldots)&=G^{\mu\mu}(\mathbf{q})\ \partial_{x_1}\Phi_\mu(x_1,t_1,\ldots)\\
2i\omega_\mu\partial_{t_1}\Psi_\mu(x_1,t_1,\ldots)&=G^{\mu\mu}(\mathbf{q}')\ \partial_{x_1}\Psi_\mu(x_1,t_1,\ldots)
\end{aligned}\tag{71}$$

with

$$G^{\mu\mu'}(\mathbf{k}')=-i\sum_{\alpha\beta\boldsymbol{\Delta}}V_{\alpha\beta}(\Delta)\Delta_x\sin(\mathbf{k}'\boldsymbol{\Delta})\,T_{\alpha\mu}(\mathbf{k}')\,T_{\beta\mu'}(\mathbf{k}').\tag{72}$$

It can be easily shown that

$$G^{\mu\mu}(\mathbf{k}')=-2i\omega_\mu(\mathbf{k}')v_\mu(\mathbf{k}')\tag{73}$$

where $v_\mu=\dfrac{\partial\omega_\mu}{\partial k_x}$ is the harmonic group velocity along the x-direction [37]. Equations (71) can be fulfilled if we assume that Φ_μ and Ψ_μ depend on the slow time scale t_1 and slow space scale x_1 only through the traveling wave variable $z_1=x_1-v_\mu t_1$.

There is also a contribution in the sum (69) originating from the other branch $\mu'\neq\mu$, which corresponds

$$\partial_{t_0t_0}u_{3,\alpha}(\mathbf{n}_0,t_0,\dots)-\sum_{\boldsymbol{\Delta}\beta}V_{\alpha\beta}(\Delta)\left(u_{3,\beta}(\mathbf{n}_0-\boldsymbol{\Delta},t_0,\dots)-u_{3,\beta}(\mathbf{n}_0,t_0,\dots)\right)= \tag{67}$$
$$-2\partial_{t_0t_1}u_{2,\alpha}(\mathbf{n}_0,t_0,\dots)-(\partial_{t_1t_1}+2\partial_{t_0t_2})u_{1,\alpha}(\mathbf{n}_0,t_0,\dots)$$
$$+\sum_{\boldsymbol{\Delta}\beta}V_{\alpha\beta}(\Delta)\Big[-\Delta_x\partial_{x_1}u_{2,\beta}(\mathbf{n}_0-\boldsymbol{\Delta},t_0,\dots)-\Delta_x\partial_{x_2}u_{1,\beta}(\mathbf{n}_0-\boldsymbol{\Delta},t_0,\dots)$$
$$+\tfrac{1}{2}\Delta_x^2\partial_{x_1x_1}u_{1,\beta}(\mathbf{n}_0-\boldsymbol{\Delta},t_0,\dots)\Big]$$
$$+\sum_{\Delta\beta\gamma}2V_{\alpha\beta\gamma}(\Delta)\Big[(u_{1,\beta}(\mathbf{n}_0-\boldsymbol{\Delta},t_0,\dots)-u_{1,\beta}(\mathbf{n}_0,t_0,\dots))$$
$$\times(u_{2,\gamma}(\mathbf{n}_0-\boldsymbol{\Delta},t_0,\dots)-u_{2,\gamma}(\mathbf{n}_0,t_0,\dots))$$
$$-\Delta_x\left(u_{1,\beta}(\mathbf{n}_0-\boldsymbol{\Delta},t_0,\dots)-u_{1,\beta}(\mathbf{n}_0,t_0,\dots)\right)$$
$$\times\partial_{x_1}u_{1,\gamma}(\mathbf{n}_0-\boldsymbol{\Delta},t_0,\dots)\Big]$$
$$+\sum_{\Delta\beta\gamma\delta}V_{\alpha\beta\gamma\delta}(\Delta)\Big[(u_{1,\beta}(\mathbf{n}_0-\boldsymbol{\Delta},t_0,\dots)-u_{1,\beta}(\mathbf{n}_0,t_0,\dots))$$
$$\times(u_{1,\gamma}(\mathbf{n}_0-\boldsymbol{\Delta},t_0,\dots)-u_{1,\gamma}(\mathbf{n}_0,t_0,\dots))$$
$$\times(u_{1,\delta}(\mathbf{n}_0-\boldsymbol{\Delta},t_0,\dots)-u_{1,\delta}(\mathbf{n}_0,t_0,\dots))\Big].$$

to the correction proportional to the space derivative introduced on the r.h.s. of equation (23):

$$B^{\mu'}_{\mathbf{k}'}(z_1,\dots)=\frac{G^{\mu\mu'}(\mathbf{q})}{\omega_\mu^2-\omega_{\mu'}^2(\mathbf{q})}\,\delta_{\mathbf{k}',\mathbf{q}}\;(1-\delta_{\mu'\mu})\,\partial_{z_1}\Phi_\mu(z_1,\dots)$$
$$+\frac{G^{\mu\mu'}(\mathbf{q}')}{\omega_\mu^2-\omega_{\mu'}^2(\mathbf{q}')}\,\delta_{\mathbf{k}',\mathbf{q}'}\;(1-\delta_{\mu'\mu})\,\partial_{z_1}\Psi_\mu(z_1,\dots). \tag{74}$$

For the second harmonic we obtain

$$B^{\mu'(2)}_{\mathbf{k}'}(z_1,\dots)=\frac{1}{2}\frac{W_{\mu\mu\mu'}(\mathbf{q},\mathbf{q},2\mathbf{q})}{\omega_{\mu'}^2(2\mathbf{q})-4\omega_\mu^2}\,\delta_{\mathbf{k}',2\mathbf{q}}\,\Phi_\mu^2(z_1,\dots)$$
$$+\frac{1}{2}\frac{W_{\mu\mu\mu'}(\mathbf{q}',\mathbf{q}',2\mathbf{q}')}{\omega_{\mu'}^2(2\mathbf{q}')-4\omega_\mu^2}\,\delta_{\mathbf{k}',2\mathbf{q}'}\,\Psi_\mu^2(z_1,\dots)$$
$$+\frac{W_{\mu\mu\mu'}(\mathbf{q},\mathbf{q}',\mathbf{q}+\mathbf{q}')}{\omega_{\mu'}^2(\mathbf{q}+\mathbf{q}')-4\omega_\mu^2}\,\delta_{\mathbf{k}',\mathbf{q}+\mathbf{q}'}\,\Phi_\mu(z_1,\dots)\Psi_\mu(z_1,\dots) \tag{75}$$

which is equal to equation (27).$W_{\mu\mu'\mu''}(\mathbf{k},\mathbf{k}',\mathbf{k}'')$ is defined in equation (28).

Going to the next-higher order we obtain in $\mathcal{O}(\epsilon^3)$ the equation

See equation (67) above.

We now truncate the asymptotic expansion of the displacement (55) and put $\mathbf{u}_l$ for $l\geq 3$ to zero. Singling out the non oscillating part we get the relation

$$\partial_{z_1}\left(D_{\mu'}(z_1,\dots)+D^*_{\mu'}(z_1,\dots)\right)=\frac{R_{\mu\mu'}(\mathbf{q})}{c_{\mu'}^2-v_\mu^2}\left|\Phi_\mu(z_1,\dots)\right|^2$$
$$+\frac{R_{\mu\mu'}(\mathbf{q}')}{c_{\mu'}^2-v_\mu^2}\left|\Psi_\mu(z_1,\dots)\right|^2 \tag{68}$$

with

$$R_{\mu\mu'}(\mathbf{k}')=4\sum_{\beta\gamma\boldsymbol{\Delta}}V_{\mu'\beta\gamma}(\Delta)\Delta_x\sin^2(\frac{\mathbf{k}'\boldsymbol{\Delta}}{2})T_{\beta\mu}(\mathbf{k}')T_{\gamma\mu}(\mathbf{k}') \tag{69}$$

as the coupling parameter and

$$c_{\mu'}^2=\frac{1}{2}\sum_{\boldsymbol{\Delta}}V_{\mu'\mu'}(\Delta)\Delta_x^2 \tag{70}$$

is the square of the sound velocity in x-direction.

Looking at the equation proportional to the first harmonic $e^{-i\omega_\mu t_0}$ and inserting equations (74, 75, 68) we eventually end up in a set of *coupled Nonlinear Schrödinger Equations* for the envelope functions Φ_μ and Ψ_μ:

$$-2i\omega_\mu\partial_{t_2}\Phi_\mu(z_1,\dots)-2i\omega_\mu v_\mu\,\partial_{x_2}\Phi_\mu(z_1,\dots)=$$
$$\omega_\mu\frac{\partial^2\omega_\mu}{\partial k_x^2}\,\partial_{z_1z_1}\Phi_\mu(z_1,\dots)+B_{11}\;\left|\Phi_\mu(z_1,\dots)\right|^2\;\Phi_\mu(z_1,\dots)$$
$$+B_{12}\;\left|\Psi_\mu(z_1,\dots)\right|^2\;\Phi_\mu(z_1,\dots).$$
$$-2i\omega_\mu\partial_{t_2}\Psi_\mu(z_1,\dots)-2i\omega_\mu v_\mu\,\partial_{x_2}\Psi_\mu(z_1,\dots)=$$
$$\omega_\mu\frac{\partial^2\omega_\mu}{\partial k_x^2}\,\partial_{z_1z_1}\Psi_\mu(z_1,\dots)+B_{12}\;\left|\Phi_\mu(z_1,\dots)\right|^2\;\Psi_\mu(z_1,\dots)$$
$$+B_{22}\;\left|\Psi_\mu(z_1,\dots)\right|^2\;\Psi_\mu(z_1,\dots) \tag{71}$$

with

$$B_{11} = \sum_{\mu'} \frac{1}{2} \frac{|W_{\mu\mu\mu'}(\mathbf{q},\mathbf{q},2\mathbf{q})|^2}{\omega^2_{\mu'}(2\mathbf{q}) - 4\omega^2_{\mu}} + \sum_{\mu'} \frac{R^2_{\mu\mu'}(\mathbf{q})}{c^2_{\mu'} - v^2_{\mu}} - 3W_{\mu\mu\mu\mu}(\mathbf{q},\mathbf{q},\mathbf{q},\mathbf{q})$$

$$B_{22} = idem\ (\mathbf{q} \to \mathbf{q}')$$

$$B_{12} = \sum_{\mu'} \frac{|W_{\mu\mu\mu'}(\mathbf{q},\mathbf{q}',\mathbf{q}-\mathbf{q}')|^2}{\omega^2_{\mu'}(\mathbf{q}-\mathbf{q}')} + \sum_{\mu'} \frac{|W_{\mu\mu\mu'}(\mathbf{q},\mathbf{q}',\mathbf{q}+\mathbf{q}')|^2}{\omega^2_{\mu'}(\mathbf{q}+\mathbf{q}') - 4\omega^2_{\mu}} + \sum_{\mu'} \frac{R_{\mu\mu'}(\mathbf{q}) R_{\mu\mu'}(\mathbf{q}')}{c^2_{\mu'} - v^2_{\mu}} - 6W_{\mu\mu\mu\mu}(\mathbf{q},\mathbf{q},\mathbf{q}',\mathbf{q}'). \quad (72)$$

By transforming the system into the reference frame moving with velocity v_μ we can drop the terms proportional to $\partial_{x_2}\Phi_\mu$ and $\partial_{x_2}\Psi_\mu$. The resulting equations are identical to equation (37).

References

1. M. Wadati, J. Phys. Soc. Jpn **38**, 673 (1975).
2. M. Toda, *Theory of Nonlinear Lattices* (Springer Verlag, Berlin-Heidelberg-New York, 1981), p. 5332.
3. E. Jackson, A. Mistriotis, J. Phys. C **1**, 1223 (1989).
4. F. Mokross, H. Büttner, J. Phys. C **16**, 4539 (1983).
5. F. Mertens, H. Büttner, in *Solitons*, edited by S. Trullinger, V. Zakharov, V. Pokrovskii (North Holland, Amsterdam, 1986).
6. N. Flytzanis, S. Pnevmatikos, M. Remoissenet, J. Phys. C **18**, 4603 (1985).
7. J. Eilbeck, in *Nonlinear Coherent Structures in Physics and Biology*, edited by M. Remoissenet, M. Peryrard (Springer Verlag, New York - Heidelberg - Berlin, 1991).
8. D. Duncan, J. Eilbeck, C. Walshaw, V. Zakharov, Phys. Lett. A **158**, 107 (1991).
9. O. Druzhinin, L. Ostrovskii, Phys. Lett. A **160**, 357 (1991).
10. Y. Kivshar, Phys. Rev. B **43**, 3493 (1991).
11. J. Pouget, M. Remoissenet, J. Tamga, Phys. Rev. B **47**, 14 866 (1993).
12. D. Bonart, A. Mayer, U. Schröder, Phys. Rev. E **51**, 13739 (1995).
13. Y. Gaididei, N. Flytzanis, F. Mertens, Physica D **82**, 229 (1995).
14. J.C. Eilbeck, presentation at *Solitons and Coherent Structures in Physics and Biology* (SOLPHYS), Technical University of Denmark, Lyngby, 1997.
15. R. Huß, F. Mertens, Y. Gaididei, in *Fluctuation Phenomena: Disorder and Nonlinearity*, edited by A. Bishop, S. Jiménez, L. Vázquez (World Scientific, Singapore, 1995), p. 244.
16. M. Lax, *Symmetry principles in solid state and molecular physics* (J. Wiley and Sons, New York-London-Sydney-Toronto, 1974).
17. M. Lighthill, J. Inst. Math. Appl. **1**, 219 (1965).
18. A. Berkhoer, V. Zakharov, Sov. Phys. JETP **31**, 486 (1970), [Zh. Exp. Teor. Fiz. **58**, 903 (1970)].
19. K. Das, S. Sihi, J. Plasma. Phys. **21**, 183 (1979).
20. M. Gupta, B. Som, B.D. Gupta, J. Plasma. Phys. **25**, 499 (1981).
21. V. Mezentsev, G. Smirnov, Opt. Commun. **68**, 153 (1988).
22. D. Benney, A. Newell, J. Math. Phys. **46**, 133 (1967).
23. V. Zakharov, E. Schulman, Physica D **4**, 270 (1982).
24. V. Zakharov, A. Shabat, Sov. Phys. JETP **34**, 62 (1972).
25. S. Manakov, Sov. Phys. JETP **38**, 248 (1974).
26. T. Ueda, W. Kath, Phys. Rev. A **42**, 563 (1990).
27. D. Kaup, B. Malomed, R. Tasgal, Phys. Rev. E **48**, 3049 (1993).
28. J. Bhatka *et al.*, Phys. Rev. E **49**, 3376 (1994).
29. M. Haelterman, A. Sheppard, Phys. Rev. E **49**, 3376 (1994).
30. Y. Silberberg, Y. Barad, Opt. Lett. **20**, 246 (1995).
31. J. Yang, D. Benney, Stud. Appl. Math. **96**, 111 (1996).
32. D. Duncan, C. Walshaw, J. Wattis, in *Nonlinear coherent structures in physics and biology*, edited by M. Remoissenet, M. Peyrard (Springer Verlag, New York - Heidelberg - Berlin, 1991), pp. 151–158.
33. E.M. Wright, G.I. Stegeman, S. Wabnitz, Phys. Rev. A **40**, 4455 (1989).
34. C.R. Menyuk, Opt. Lett. **12**, 614 (1987).
35. C.R. Menyuk, J. Opt. Soc. Am. B **5**, 392 (1988).
36. V.V. Afanasyev, Y.S. Kivshar, V.V. Konotop, V.N. Serkin, Opt. Lett. **14**, 805 (1989).
37. V.V. Konotop, Phys. Rev. E **53**, 2843 (1996).